HYDROGEN GAS SENSING OF ZnO NANOWIRES SYNTHESIS BY HYDROTHERMAL TECHNIQUE

M. JABEEN[a*], M. W. ASHRAF[b], S. TAYYABA[c], S. MANZOOR[d],
M. T. JAVED[e], R. V. KUMAR[f], M. AHMED[g]
[a]*Government Degree College for Women Haveli Lakha, District Okara, Punjab, Pakistan*
[b]*Department of Physics (electronics) GC University, Lahore, Pakistan*
[c]*Department of Computer Engineering, The University of Lahore, Lahore, Pakistan*
[d]*Department of Physics, University of the Punjab Lahore*
[e]*Office of Research Innovation and Commercialization, Pakistan Institute of Engineering and Applied sciences, Nilore, Islamabad, Pakistan*
[f]*Department of Material Science and Metallurgy, University of Cambridge United Kingdom*
[g]*Department of Physics, University of the Sargodha Lahore Campus, Lahore, Pakistan*

Zinc oxide nanowires were synthesized by simple hydrothermal method at 65^oC for 12 hour. We have used the neutrient solution of zinc-nitrate $((Zn(NO_3)_2)$ with hexamethylene tetramine $(C_6H_{12}N_4)$ in equimolar ratio. Growth pattern of ZnO NWs were epitaxial and investigated by X-ray diffraction for crystal structure that shows the zinc oxide nanowires are in hexagonal (wurtzite) structure form. UV-visible photometer spectro calculate the absorption (amalgamation) spectrum of zinc oxide nanowires. The surface morphology of as synthesized zinc oxide nanowires was measured by Field Emission Scanning Electron Microscopy (FE-SEM). The sensor manufactured by zinc oxide (ZnO) nanowires grown by hydrothermal technique was utilized for hydrogen gas sensing at 150^oC for about 1000 ppm concentration. The detector manufacture for hydrogen sensing shows a reversible cycle. The affect of working temperature was also tested on hydrogen gas sensing properties of ZnO nanowires.

1. Introduction

Electronic noses are presumed like gas sensors progressively used for contaminated and combustible gases sensing [1-5]. The inner most importance has gained by the hydrogen gas due to construction of innovative unassailable energy as hygienic and capable energy resource to substitute oil dependence on accessible energy sources [6-10]. During the most recent years, various detectors for hydrogen gas sensing have been constructed that operate at different temperatures. Gas detectors that depend on solid state such as semiconductor metal oxide have wide band-gap applications shows much consistency for gas detection. At present, controlled parameters for the construction of semiconductor metal oxide nanostructures such as their organized dimension, size and shape has paying much attention for their appealing and exceptional properties. Such parameters involve chemical, optical, electronic and detection properties [11]. ZnO is intrinsically an n-type metal oxide with fascinating properties. It has 3.37 eV band-gap and lie in the range of wide bandgap semiconductor materials. ZnO has 60 meV binding energy values

---

*Corresponding author: musarrat97@yahoo.com

that are large enough at room temperature. Thus complimentary UV applications belong to ZnO [12-13]. Additionally, we can synthesize nanostructures such as nanowires, nanorods from ZnO with high aspect-ratio (surface to volume ratio). Sensor that detects various kinds of reducing gases can be manufactured from these nanostructures with high aspect ratio [14-15]. Nanostructures show much sensitivity response and selectivity for sensing different gases at low temperature than bulk materials from them thin film gas detectors are constructed [16-18]. Gas detectors that operate at low temperature show different compensation [19-22] like long-life, secure and low power consumption. At the present time scientists are trying to manufacturer sensors from those materials that work at low temperature situation [23]. Sensors that are constructed from ZnO nanowires array via hydrothermal technique which is a striking development. Hydrothermal process is an economical and most simple method to synthesize nanowires array [24-25]. Doping of various materials especially, Pd and Pt also enhance the sensitivity and response of the hydrogen gas [26-31].

2. Experimental detail

All the chemical purchase from Sigma Aldrich U.K was of analytical grade with 99.9 % purity. ZnO nanowires were synthesized from hydrothermal technique. A substrate was cleaned from standard method using de-ionized water, ethanol, acetone and then dried to eliminate all the impurities. The substrate then dipped in dodecanethiol solution of 1% in ethanol for adhesion of nanowires on the surface of substrate. We prepared solution of zinc acetate in ethanol 0.01 molar for seeding film (few micrometers thickness). We dry the substrate on a hotplate at 60°C for 5 min. The substrate was inverted in 10mM equimolar neutrient solution of zinc nitrate hex-hydrate and hexamethylenetetramine (($CH_2)_6N_4$) at 80°C temperature for 12 h. After each 3 hours solution was changed for better growth of ZnO nanowires. Post annealing is essential for the elimination of all the impurities like organic and chemical vapors.

3. Findings and argument

3.1. Crystal structure analysis by X-ray diffraction

Graph shows intensity versus 2θ position taken from 20 to 60 on x-axis. It is also confirm from the graph that all the ZnO peaks are present that corresponds to (1 0 0), (0 0 2) and (0 0 1) position. The crystal structure of hexagonal ZnO nanowires as shows in Fig.1 have indices a, b and c with a=b=3.2490, and c=90. We have used the copper kα-radiations [Space group number p63mc (186) with pattern 1993].
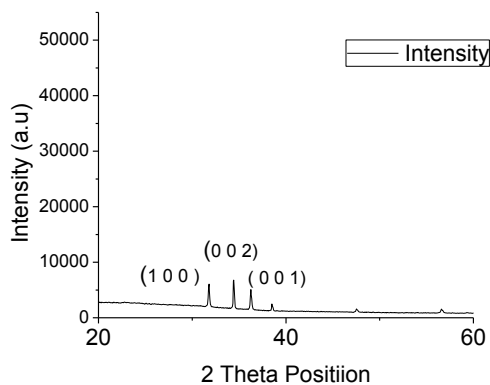
Fig. 1. Intensity versus 2θ position of zinc oxide nanowires grown by hydrothermal process.

3.2. Surface morphology of hexagonal ZnO nanowires by FE-SEM

Zinc oxide (ZnO) nanowires have flower like surface morphology [32] as investigated with Field Emission Scanning Electron Microscope (JSM-6340F). ZnO nanowires have high aspect ratio and hexagonal wurtzite structure shows in Fig-2. This imagery was taken at a magnification ×50,000, ×18000, ×15,000 and× 23,000. We operate the machine at 30 KeV. All the images were recorded with SEI mode. We used WD=9 in the standard mode of display.
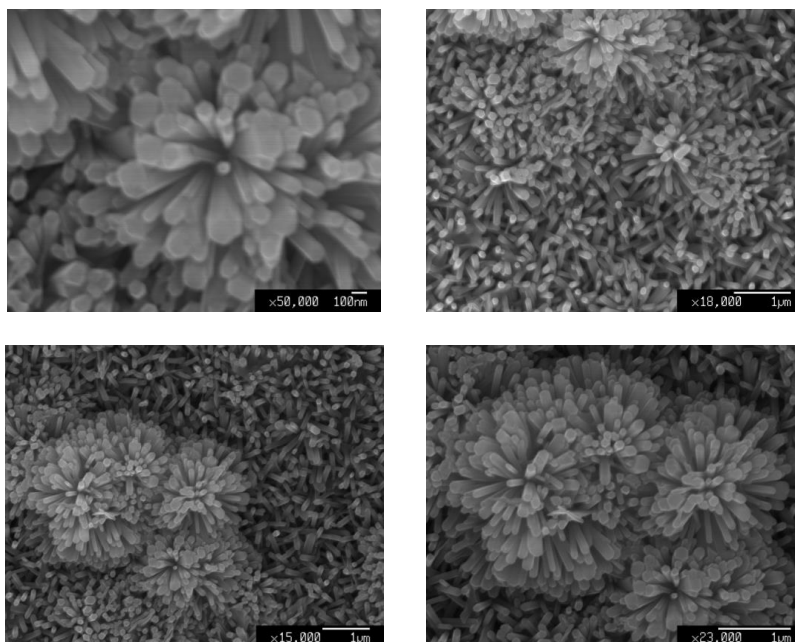
Fig. 2. Images of ZnO nanowires by FESEM grown by hydrothermal technique on FTO
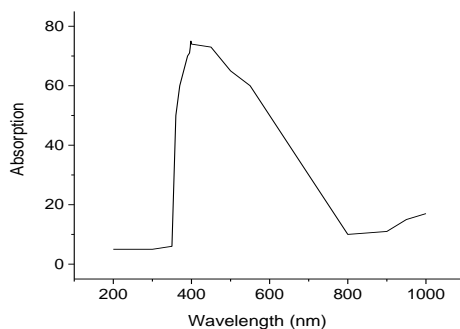
Fig.3. UV-visible spectra of ZnO nanowires measured with Lambda-750

Fig.-3 shows absorption spectra of zinc oxide nanowires. Nanowires top most peak at 380 nm in the wavelength range [33]. ZnO is a wide band-gape material with a value 3.30 eV. The spectrum of ZnO related to its exaction binding energy limit. Its inferior limit related to valance band of donor transition range. Amalgamation (absorption) pattern of ZnO nanowires was determined. ZnO absorption spectra have a wide range because of existence of defects. ZnO has excellent crystal structure due to defects and sharpness of the peak.

4. Nanowires synthesis method

Equimolar neutrient solution of hexamethylene tetramine ($C_6H_{12}N_4$ (HMTA) with zinc-nitrate (($Zn(NO_3)_2$)) tear up because of the process of ion development (Zn^{2+} and OH^-) with increase in temperature. The nuclei of ZnO formed in the solution at small absorption of zinc-nitrate (($Zn(NO_3)_2$)) and hexamethylene tetramine ($C_6H_{12}N_4$ chemicals. HMTA is accountable for hexagonal phase of ZnO nanowires. Synthesis of ZnO nanowires depends upon the kinetic-growth process and parameters of nucleation. Hydroxide ions are created by HMTA with ammonium molecules in neutrient solution [34]. Whil the surface scrutinize pattern of hexagonal ZnO nanowires was determined by zinc (II) $[Zn(NH_3)_4]^{2+}$ and $[Zn(OH)_4]^{2-}$

Hexagonal ZnO nanowires reaction process is given below:

$$Zn^{2+} + 4OH^- \rightarrow [Zn(OH)_4]^{2-} \tag{1}$$

$$Zn^{2+} + 4NH_3 \rightarrow [Zn(NH_3)_4]^{2+} \tag{2}$$

$$[Zn(NH3)4]^{2+} + 2OH \rightarrow ZnO + 4NH_3 + H_2O \tag{3}$$

$$[Zn(OH)_4]^{2-} \rightarrow ZnO + H_2O + 2OH^- \tag{4}$$
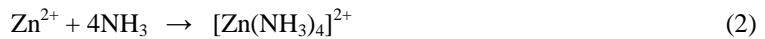
4.1. Hydrogen Gas detection technique

Pt contacts were applied on the active surface of the sensor with sputter coater EMITECH K-575 for hydrogen detection [35]. Gas detector was kept in the test chamber. ZnO nanowires has high aspect-ratio to react with hydrogen gas. The conductivity of ZnO nanowires varies with the variation in depletion-region. ZnO nanowires absorbs O_2 the ambient air, so resistivity increased. Due to such kind of process oxygen (O_2) ions eradicate electrons at various temperatures. This mechanism takes place in the conduction band of zinc oxide nanowires. Conductance increased in semiconductor metal-oxides by increase in temperature. Oxygen species transfer oxygen ions (O^- O^{2-} O_2^-) [36-37]. Chemically, O_2 atom immersed on ZnO active surface. Reaction mechanism is given below:

$$O_2 + e^- \leftrightarrow O_2^- \tag{a}$$

For low temerature conditions the liberated electrons captured in oxygen molecules (O_2). Then oxygen ions created through the given method:

$$O_2 + 2e^- \leftrightarrow O^- \tag{b}$$

Hence charge carrier concentration decreased with the production of depletion film produced on the active surface of the sensor.

$$O_2 + 4e^- \leftrightarrow O^{2-} \tag{c}$$

Hydrogen gas (H_2) separated at O_2 position on the surface of ZnO nanowire sensor. Zinc oxide is intrinsically an n-type semiconductor substance. Conductance increased through reducing gases reaction [38]. Consequently, hydrogen atoms facilitated due to reaction with hydrogen and immersed (absorbed) oxygen gas. Hence, the conductivity of the sensor increased with the production of O_2 chemisorbed electrons from conduction band zinc oxide [39-40].

The following reactions take place at low and high temperature on the active surface of oxygen:

$$O^- + 2H_2 \rightarrow H_2O_{(gas)} + e^- \tag{d}$$

$$O_{2+2}H_2 \rightarrow 2H_2O + e^-, \quad \text{(low down temperature)} \tag{e}$$

$$O^- + H_2 \rightarrow H_2O + e^-, \quad \text{(Elevated temperature)} \tag{f}$$
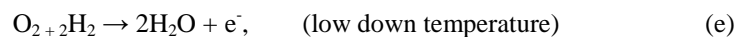
Change in resistivity or conductivity with the flow of reducing gas in electrochemical detectors shows sensitivity of the sensor that write in the type of % sensitivity [41-42].

$$S(\%)= [(\ R_{gas} - R_{air})/R_{air}]\times 100$$

The experimental consequences show that resistance reduced with increasing temperature and absorption of reducing gas species. Detection process of the hydrogen gas at 150°C with 1000 ppm shows in Fig-4. The flow of hydrogen gas with 1000 ppm through the detector shows a reversible behavior in ambient air circumstances.

Additionally resistance decrease in 2-steps. In starting 150 s detector shows reduction behavior   and afterward a slow decrease about 350 s of (25%) of gas disclosure. Therefore, the experimental results show that resistance increased 100%   in 280 s after exclusion of hydrogen gas.
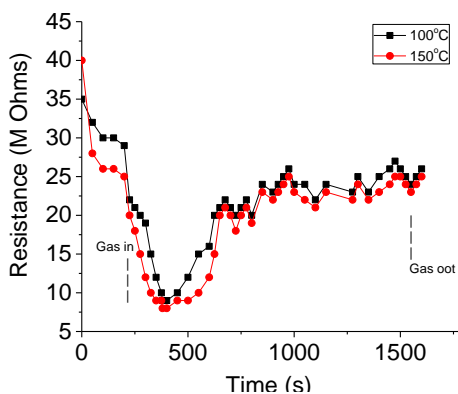
Fig. 4(a): Resistance versus time at various temperatures.

Graph 4(a) indicates that resistance decreased quickly with increase of temperature. It approximately attains a value of 8 MΩ with hydrogen gas disclosure. After the escape of hydrogen gas it yet again increases and become linear in 800 s.
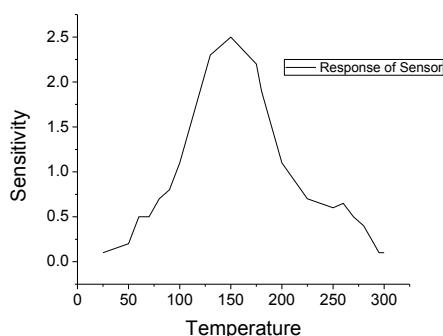
Fig. 4(b): Sensitivity versus temperature.

Fig-4(b) investigates the response versus operating temperature. To measure sensitivity temperature varies from 50 to 350°C. Sensitivity of ZnO nanowire sensor is actually the   response of the detector (S). Experimental results show that the sensitivity enhanced through increasing in temperature and gain the highest limit 2.5 at 150°C. Its value shows a decrease by means of further enhance in operating temperature of the sensor.

5. Conclusions

Pure ZnO nanowires were grown through economic and simple hydrothermal technique. Nanowires ha hexagonal wurtzite structure as confirmed from the FESEM images. Nanostructures have high aspect ratio that is the important parameter for detection of hydrogen gas at low value of temperature. Detection of hydrogen gas increased trough outstanding individuality of ZnO nanowires. Sensing of hydrogen gas is done by absorption/desorption technique on the active surface of the detector. This operation is done at low temperature circumstances.

Hydrogen detector works at ambient air situation. Its behavior is a reversible curve via disclosure of hydrogen gas. Reversible curve completes in 800 s. The experimental results show the sensitivity of the detector at various working temperatures from 50-350°C. We investigate the maximum value 2.5 of sensitivity at 150°C. Detector response and recovery-times were diminutive through increase in temperature. Hence, corresponding activation energy increases by absorption and desorption process of hydrogen gas.

Acknowledgments

References

[1] J. J. Hassan, M. A. Mahdi, C. W. Chin, H. Abu-Hassan, Z. Hassan, Journal of Alloys and Compounds **546,** 107 (2013).
[2] L. Chu, Y. Liu, H. Fu, Y. Ding, M. Gao, H. Pan, Journal of Alloys and Compounds **509**(30) 7844 (2011).
[3] T. Hübert, L. Boon-Brett, G. Black, U. Banach, Sens. Actuat. B: Chem. **157,** 329 (2011).
[4] F. Rock, N. Barsan, U. Weimar, Chem. Rev. **108,** 705 (2008).
[5] Q. Jiang, C. Wu, L. Feng, L. Gong, Z. Ye, J. Lu, Applied Surface Science **357,** 1536 (2015).
[6] Sukon Phanichphant, Procedia Engineering, **87,** 795 (2014).
[7] P. Gouma, S. Sood, M. Stanacevic, S. Simon, Procedia Engineering **87,** 9 (2014).
[8] A. Hastir, N. Kohli, R. C. Singh, Journal of Physics and Chemistry of Solids **105,** 23 (2017).
[9] X. Wu, , S. Xiong, , Z. Mao, Y. Gong, W. Li, B. Liu, S. Hu, X. Long, Journal of Alloys and Compounds **704**(15), 117 (2017).
[10] K. Hassan, A.S.M. Iftekhar Uddin, F. Ullah, Y. S. Kim and G-S. Chung, Materials Letters **176,** 232 (2016).
[11] T. Li, W. Zenga, Z. Wang, Sensors and Actuators B **221,** 1570 (2015).
[12] L. Feng, A. Liu, M. Liu, Y. Ma, J. Wei, B. Man, Journal of Alloys and Compounds **492,** 427 (2010).
[13] P. Ooi, S. Lee, S. Ng, Z. Hassan, H. A. Hassan, Journal of Materials Science & Technology, **27**(5), 465 (2011).
[14] J. M. Jang, C. R. Kim, H. Ryu, M. Razeghi, W. G. Jung, J. Alloys Compd. **463**, 503 (2008).
[15] J. Karamdel, C.F. Dee, K.G. Saw, B. Varghese, C.H. Sow, I. Ahmad, B.Y. Majlis, J.Alloys Comp. **512**, 68 (2012).
[16] K. Mirabbaszadeh and M. Mehrabian, Phys. Scr. **85**, 035701 (2012).
[17] C. Liangyuan, L. Zhiyong, B. Shouli, Z. Kewei, L. Dianqing, C. Aifan, C.C. Liu, Sens. Actuat. B: Chem. **143**, 620 (2010).
[18] J. Chen, J. Li, J. Li, G. Xiao, X. Yang, J. Alloys Comp. **509**, 740 (2011).
[19] S. D. Shinde, G. E. Patil, D. D. Kajale, V. B. Gaikwad, G. H. Jain, J. Alloys Comp.

528, 109 (2012).

[20] H.-Y. Lee, H.-L. Huang, C.-T. Lee, Sens. Actuat. B: Chem. **157**, 460 (2011).

[21] J. S. Wright, W. Lim, D. P. Norton, S. J. Pearton, F. Ren, J. L. Johnson, A. Ural, Semicond. Sci. Technol. **25**, 024002 (2010).

[22] M. W. Ahn, K. S. Park, J. H. Heo, J. G. Park, D. W. Kim, Appl. Phys. Lett. **93**, 263103 (2009).

[23] K. J. Choi, H. W. Jang, Sensors **10**, 4083 (2010).

[24] S. N. Das, J.P. Kar, J. H. Choi, T. I. Lee, k. j. Moon, J. M. Myoung. The Journal of Physical Chemistry C, **114**(3), 1689 (2010).

[25] M. H. Huang, Y. Wu, H. Feick, N. Tran, E. Weber, P. Yang, Catalytic Growth of Zinc Oxide Nanowires by Vapor Transport, **13**(2), 113 (2001).

[26] H. T. Wang, B. S. Kang, F. Ren, L. C. Tien, P. W. Sadik, D. P. Norton, S. J. Pearton, J. Lin, Appl. Phys. A **81**, 1117 (2005).

[27] S. Ren, G. Fan, S. Qu, Q. Wang, J. Appl. Phys. **110,** 084312 (2011).

[28] L. C. Tien, P. W. Sadik, D. P. Norton, L. F. Voss, S. J. Pearton, H. T. Wang, B. S. Kang, F. Ren, J. Jun, J. Lin, Appl. Phys. Lett. **87,** 222106 (2005).

[29] F. C. Huang, Y. Y. Chen, T. T. Wu, Nanotechnology **20**, 065501 (2009).

[30] Q. A. Drmosh, Z.H. Yamani, Applied Surface Science **375**, 57 (2016).

[31] R. Yatskiv, J. Grym, P. Gladkov, O. Cernohorsky, J. Vanis, J. Maixner, J. H. Dickerson, Solid-State Electronics **116**, 124 (2016).

[32] T. Wang, X. Kou, L. Zhao, P. Sun, C. Liu, Y. Wang, K. Shimanoe, N. Yamazoe, G. Lu, Sensors and Actuators B: Chemical **250**, 692 (2017) .

[33] V. Srikant, D. R_ Clarke. Journal of Applied Physics **83**(10), 5447 (1998).

[34] H. Zhang., D. Yang., D. Li., X. Ma., S. Li, D. Que., Crystal growth & design **5**(2), 547 (2005).

[35] D-T. Phan, A.S.M. Iftekhar Uddin, G-S. Chung, Sensors and Actuators B **220,** 962 (2015).

[36] A. B. Bodade., A. M. Bende, and G. N. Chaudhari, Vacuum **82**(6), 588 (2008).

[37] M. F. B Alam., D. T. Phan., & G. S. Chung, Materials Letters **156,** 113 (2015).

[38] V. Galstyann, E. Comini, C. Baratto, G. Faglia and G. Sberveglieri, Ceramics International **41**, 14239 (2015).

[39] A. D. S. Basu, Mater. Chem. Phys. **47,** 93 (1997).

[40] M. Cittadini, M. Sturaroa, M. Guglielmi, A. Resmini, I.G. Tredici, U. Anselmi-Tamburini, P. Koshy, C.C. Sorrell, A. Martucci, Sensors and Actuators B **213,** 493 (2015).

[41] N. S. Ramgir, M. Ghosh, P. Veerender, N. Datta, M. Kaur, D.K. Aswal, S. K. Gupta, Sens. Actuat. B: Chem. **156**, 875 (2011).

[42] R. D. Ladhe., K. V. Gurav, S. M. Pawar, J. H. Kim, B. R. Sankapal, Journal of Alloys and Compounds **515,** 80 (2012).